ELSEVIER

Ceramics International 28 (2002) 165–169

CERAMICS INTERNATIONAL

www.elsevier.com/locate/ceramint

Synthesis of nickel nanoparticles dispersed in γ-alumina by heterogeneous precipitation

Guo-Jun Li*, Xiao-Xian Huang, Meiling Ruan, Jing-Kun Guo

Shanghai Institute of Ceramics, Chinese Academy of Sciences, 1295 Ding-Xi Road, Shanghai 200050, People's Republic of China

Received 7 January 2001; received in revised form 10 April 2001; accepted 12 June 2001

Abstract

A heterogeneous precipitation method is described for obtaining nanocomposite powders consisting of Ni nanoparticles homogeneously dispersed within γ-Al_2O_3. The amorphous $Al(OH)_3$ was nucleated on the surfaces of NiO nanoparticles and crystallized to γ-Al_2O_3 at 900 °C. The porosity of γ-Al_2O_3 allowed the growth of NiO nanoparticles during calcinations. After the calcined nanocomposite powders were selectively reduced at 700 °C in a hydrogen atmosphere, NiO nanoparticles were converted to Ni with the size of 25–35 nm. TEM observation and AES analysis showed Ni nanoparticles were uniformly dispersed in the γ-Al_2O_3 matrix.

Keywords: A. Grain growth; A. Powders: chemical preparation; B. Nanocomposites; D. Al_2O_3

1. Introduction

Ceramics are used in many fields. However, the utility of a ceramic material in an engineering application is critically determined by its brittleness. Thus, the toughening of ceramic materials is very necessary. The dispersion of a ductile metallic phase (Ni, W, Cr, Cu etc.) in a brittle ceramic matrix is found to be a promising way [1–4]. Reinforcement models show the importance of the homogeneity and the small size of the metallic inclusion [5]. So the synthesis of good composite powders is very important for preparing good properties of materials. The control of the microstructure of ceramic–metal composites is generally difficult to achieve by traditional techniques involving mechanical mixing of ceramic and metallic powders followed by hot pressing [6,7]. A small-scale homogeneity can be obtained using the sol-gel route [8–10]. However, the relatively high cost of some reactants and the difficulty to control the gel drying step are drawbacks to this method. The heterogeneous precipitation method is a promising way because of inexpensive raw materials and simple processing. A large number of studies have been done and have obtained exciting results [11,12].

In the present work, γ-Al_2O_3–Ni nanocomposite powders were prepared by the heterogeneous precipitation method. The purpose of this paper is to explain the expectation of obtaining a much better microstructure and property of material.

2. Experimental procedures

γ-Al_2O_3–Ni composite powders were prepared using NiO [with the average size of 8 nm (SICCAS, China)], $Al(NO_3)_3{\cdot}9H_2O$ (analytically pure) and $NH_3{\cdot}H_2O$ as the starting materials. NiO powders which were equivalent to 12.5 wt.% $Al(NO_3)_3{\cdot}9H_2O$ were dispersed in 0.02 M $Al(NO_3)_3{\cdot}9H_2O$ solution by sonication Poly-ethylene glycol (PEG, molecular weight 1500) (2 wt.%, equivalent to NiO weight) solution was used as dispersant to prevent NiO powders agglomerating. Next, 1 M $NH_3{\cdot}H_2O$ solution under vigorous stirring was added dropwise to the homogeneous slurry obtained above. To ensure complete reaction, an excess of $NH_3{\cdot}H_2O$ was used and the pH value of the mixed solution was adjusted to 9 during precipitation. The resulting precipitates were filtered and thoroughly washed three times with distilled water. Finally, the precipitates were dried at 70 °C for 24 h. The as-dried precipitates were calcined in air at 700 and 900 °C for 2 h at a heating rate of 5 °C/min and

* Corresponding author. Fax: +86-21-6251-3903.
E-mail address: guojunlee@netease.com (G.-J. Li).

0272-8842/02/$22.00
PII: S0272-8842(01)00073-6

the samples were calcined at 900 °C and reduced at 700 °C for 4 h in a hydrogen atmosphere at a heating rate of 5 °C/min.

The thermal decomposition behavior of as-precipitated composite powders was studied by thermogravimetric analysis (TGA) and differential thermal analysis (DTA) on a Netzsch-STA 429 thermal analysis device. TGA–DTA determination was carried out in air in an Al_2O_3 crucible at a heating rate of 10 °C/min from room temperature to 1200 °C. X-ray diffraction (XRD) patterns were obtained at a scanning rate of 4°/min with 2θ range from 20 to 70° using a fully automated diffractometer (Riaku RAX-10, Japan) with CuK_α (0.15406 nm) radiation. A transmission electron microscope (TEM) (model JEM-200CX, Jeol, Tokyo, Japan) was used for investigating the particle size and the shape of the composite powders. Auger energy spectra (AES) (Microlab 310F, VG Scientific Ltd, USA) were used to investigate the state of the surface of the particles.

3. Results and discussion

The DTA and TGA curves of the as-dried composite powders shown in Fig. 1 had three exothermic peaks and one endothermic peak. From the DTA curve, it can be seen that the endothermic peak at about 140 °C was due to hydration and the exothermic peak at 290 °C was assigned to PEG burnout, which coincided with the abrupt weight losses over the temperature range from 50 to 400 °C on the TGA curve. The weak exothermic peaks at 895 and 1100 °C were associated with the amorphous $Al(OH)_3 \rightarrow \gamma$-$Al_2O_3$, γ-$Al_2O_3 \rightarrow \alpha$-$Al_2O_3$ transformations, respectively, which was proved by the XRD results shown in Fig. 2.

The composite powders dried at 70 °C for 24 h, calcined at 700, 900 and 1200 °C for 2 h in air and reduced at 700 °C for 4 h in hydrogen were identified by XRD, as shown in Fig. 2. The XRD pattern of the dried powders showed the obtained $Al(OH)_3$ was an amorphous phase because no new peaks appeared except for those of the NiO particles. When calcined at 900 and 1200 °C, the XRD appeared at diffraction peaks of γ-Al_2O_3 and α-Al_2O_3, which was in agreement with the DTA analysis. The broad γ-Al_2O_3 peaks and amorphous background suggested the existence of fine crystalline, meantime the NiO peaks of the calcined powders were sharper than those of the uncalcined powders, indicating the agglomeration and growth of NiO nanoparticles. The XRD pattern of the calcined powders reduced at 700 °C in hydrogen showed NiO particles were converted to Ni particles. Generally, the temperature of the amorphous $Al(OH)_3 \rightarrow \gamma$-$Al_2O_3$ and γ-$Al_2O_3 \rightarrow \alpha$-$Al_2O_3$ phase transformations was at 500–800 and 1150–1250 °C, respectively [13]. However, in this study, the temperature of the amorphous $Al(OH)_3 \rightarrow \gamma$-$Al_2O_3$ is near 900 °C, which shows NiO nanoparticles can retard amorphous$\rightarrow\gamma$

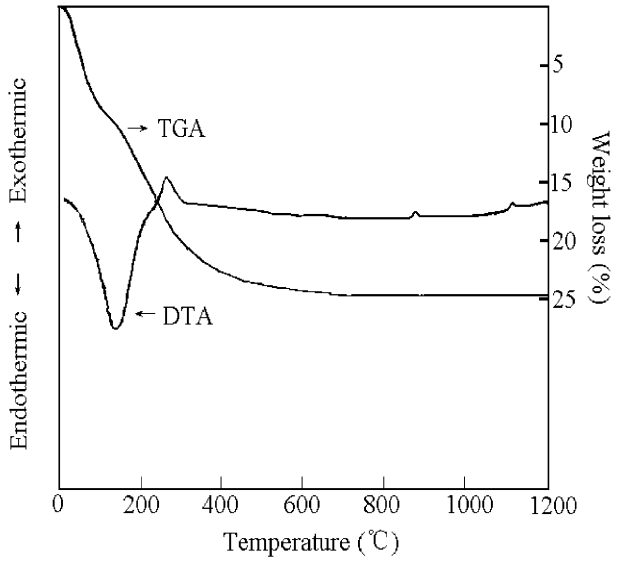

Fig. 1. The DTA and TG curves of the dried composite powders.

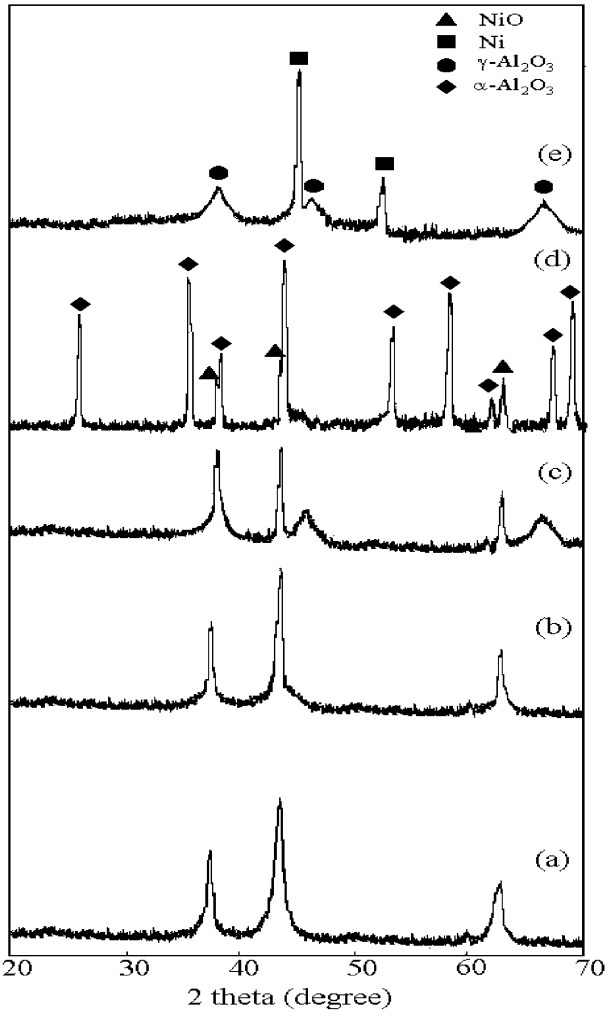

Fig. 2. XRD patterns of the composite powders: (a) dried; (b) calcined at 700 °C; (c) calcined at 900 °C; (d) calcined at 1200 °C; (e) reduced at 700 °C (after the dried composite powders were calcined at 900 °C).

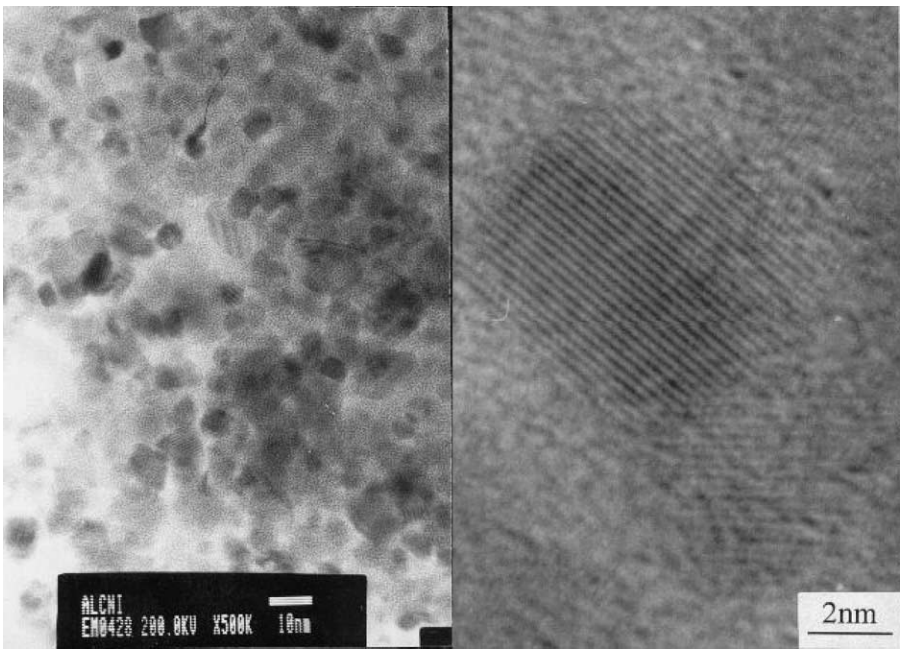

Fig. 3. TEM and HREM images of the dried composite powders.

phase transformation. The DTA and XRD results also show the effect of NiO nanoparticles on $\gamma \rightarrow \alpha$ phase transformation is small, which is in agreement with the result of Okada [14]. An amount of research [15–19] has focused on the effect of metal oxide seeds on γ-$Al_2O_3 \rightarrow \alpha$-$Al_2O_3$ phase transformation and has demonstrated that the increase or decrease of the $\gamma \rightarrow \alpha$ conversion temperature was due to the increase or reduction of the activation energy barrier. According to previous research, the increase of amorphous$\rightarrow\gamma$ transformation temperature possibly resulted from increase of the activation energy barrier involved in the thermally activated nucleation process.

The TEM and HREM images of the dried composite powders are shown in Fig. 3. The TEM image indicated the NiO particles (dark field) were uniformly dispersed in the amorphous $Al(OH)_3$. From the corresponding HREM image, it was evident that the amorphous $Al(OH)_3$ coated the surface of the NiO nanoparticles. This is a typical coated structure. The core particles are NiO particles and the shell layers are $Al(OH)_3$. The above results suggested the nuclei of $Al(OH)_3$ in the solution grew on the surfaces of NiO core particles instead of forming discrete precipitates in the presence of NiO nanoparticles. The NiO surface acted as heterogeneous nucleation sites.

The NiO nanoparticles dispersed in γ-Al_2O_3 were completely reduced to Ni at 700 °C for 4 h in an hydrogen atmosphere after the composite powders were calcined at 900 °C by XRD analysis (Fig. 2e). According to Scherrer's equation (particle is spherical):

$$D = 0.89\lambda / B\cos(\theta)$$

where D is the average particle size, B is the full-width at half-height of the peak, λ is the wavelength of X-ray and θ is the diffraction angle of the peak. The average particle size of NiO is about 31 nm; its TEM is shown in Fig. 4. As observed from TEM, the size of nanocrystalline Ni was 25–35 nm because of the agglomeration and growth of NiO particles during calcinations, which coincided with XRD results. γ-Al_2O_3 is a porous structure whose porous walls consist of a lot of single Al_2O_3 particles [20]. Such a structure may allow gas to flow freely, which is favorable to reducing NiO by hydrogen. So in this study, γ-Al_2O_3–Ni composite powders were prepared. However, the porosity of γ-Al_2O_3 allowed the

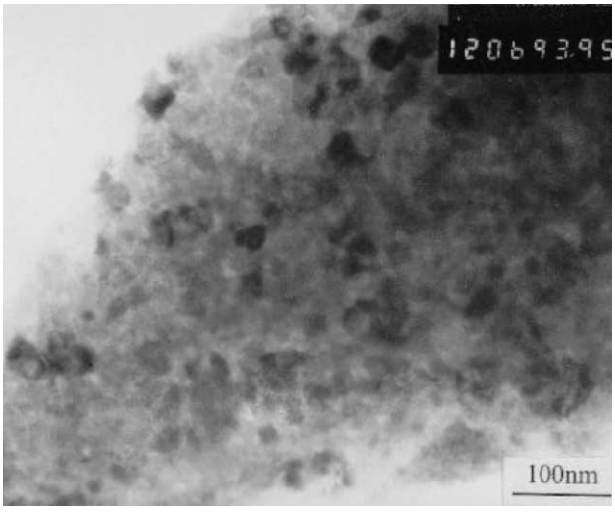

Fig. 4. TEM micrograph of the composite powders reduced at 700 °C (after the dried composite powders were calcined at 900 °C).

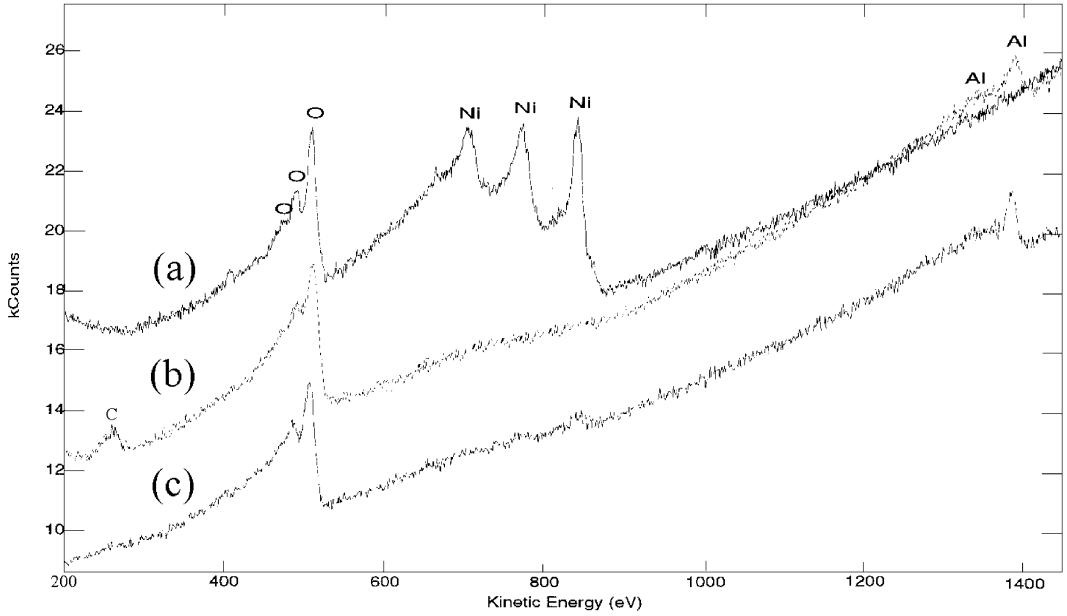

Fig. 5. AES spectra (a) as-received NiO, (b) the dried composite powders and (c) the composite powders reduced at 700 °C (after the dried composite powders were calcined at 900 °C).

growth of NiO during calcinations according to TEM observation (Fig. 4) and XRD analysis (Fig. 2c).

AES analysis was conducted on the composite powders dried and reduced after being calcined 900 °C, respectively. A blank experiment was carried out on as-received NiO powders, which was used for contrast. Their AES spectra are shown in Fig. 5. As is known, AES can provide the information about compositions of several layers of atoms (about 1 nm) on the surface of materials, so it is suitable to investigate the status of the surface of the particles. In the blank sample, only two kinds of element were detected by the AES technique (Fig. 5a). Kinetic energy at 490 and 510 eV indicated the element O auger peak, Ni peaks were near 706, 776 and 842 eV; the former two were weak peaks. However, the AES spectrum of the dried composite powders (Fig. 5b) showed element C, O and Al auger peaks were tested and no Ni auger peaks appeared. Kinetic energy of C auger peak corresponding to the organic dispersant was at 273 eV and that of Al peaks was at 1327 and 1376 eV. A reasonable inference was that the amorphous $Al(OH)_3$ was precipitated on the surfaces of NiO particles. From the spectrum of the reduced composite powders (Fig. 5c), it was observed that the C peak disappeared for the elimination of organic dispersant, but the Ni peaks had not appeared yet except for the O and Al auger peaks, indicating Ni nanoparticles were uniformly dispersed in γ-Al_2O_3.

4. Conclusion

γ-Al_2O_3–Ni nanocomposite powders were successfully prepared by the heterogeneous precipitation method using NiO, $Al(NO_3)_3{\cdot}9H_2O$ and $NH_3{\cdot}H_2O$ as the starting materials. In the presence of the NiO nanoparticles, the NiO surface acted as heterogeneous nucleation sites, so the nuclei of the amorphous $Al(OH)_3$ in slurry grew on the surface of NiO core particles. The amorphous phase were crystallized to γ-Al_2O_3 at 900 °C for 2 h in air, NiO nanoparticles in nanocomposite powders were then completely reduced to Ni at 700 °C for 4 h in an hydrogen atmosphere. TEM observation and AES analysis showed Ni nanoparticles were uniformly dispersed in the γ-Al_2O_3 matrix. In addition, NiO nanoparticles can retard the amorphous $Al(OH)_3 \rightarrow \gamma$-$Al_2O_3$ transformation, but the effect on γ-$Al_2O_3 \rightarrow \alpha$-$Al_2O_3$ transformation is small.

References

[1] W.H. Tuan, R.J. Brook, The toughening of alumina with nickel inclusions, J. Eur. Ceram. Soc. 6 (1990) 31–37.
[2] T. Sekino, K. Niihara, Fabrication and mechanical properties of fine-tungenten-dispersed alumina-based composites, J. Mater. Sci. 32 (1997) 3943–3949.
[3] S.A. Cho, M. Puerta, B. Cols, J.C. Ohep, Sintering behavior of Al_2O_3–Cr and Al_2O_3–$Cr(NO_3)_3$ mixtures, Powder Metall. Int. 12 (1980) 192–195.
[4] S.T. Oh, T. Sekino, K. Niihara, Fabrication and mechanical properties of 5 vol.% copper dispersed alumina nanocomposite, J. Eur. Ceram. Soc. 18 (1998) 31–37.
[5] A.G. Evans, High toughness ceramics, Mater. Sci. Eng. A105/106 (1988) 65–75.
[6] W.H. Tuan, R.J. Brook, Processing of alumina/nickel composites, J. Eur. Ceram. Soc. 10 (1992) 95–100.
[7] W.H. Tuan, W.B. Chou, Preparation of Al_2O_3–AlN–Ni composites, J. Am. Ceram. Soc. 80 (9) (1997) 2418–2420.
[8] E. Breval, G. Dodds, C.G. Pantano, Properties and microstructure of Ni–alumina composite materials prepared by the sol/gel method, Mater. Res. Bull. 20 (10) (1985) 1191–1205.

[9] E. Breval, Z. Deng, et al., Sol–gel prepared Ni–alumina composite materials, J. Mater. Sci. 27 (1992) 1464–1468.
[10] E.D. Rodeghiero, O.K. Tse, J. Chisaki, E.P. Giannelis, Synthesis and properties of Ni-α–Al_2O_3 composites via sol-gel, Mater. Sci. Eng. A 195 (1995) 151–161.
[11] S.W. Wang, X.X. Huang, J.K. Guo, Synthesis and characterization of yttria-stabilized tetragonal zirconia polycrystalline powder coated with silica layers, Mater. Lett. 28 (1996) 43–46.
[12] M.D. Sacks, N. Bozkurt, G.W. Scheiff, Fabrication of mullite and mullite-matrix composites by transient viscous sintering of composite powders, J. Am. Ceram. Soc. 74 (10) (1991) 2428–2437.
[13] W.H. Gitzen, Alumina as Ceramic Materials, The American Ceramic Society, Columbus, OH, 1970.
[14] K. Okada, A. Hattori, T. Taniguchi, Effect of divalent cation additives on the γ-$Al_2O_3 \rightarrow \alpha$-$Al_2O_3$ phase transition, J. Am. Ceram. Soc. 83 (4) (2000) 928–932.
[15] G.C. Bye, G.T. Simpkin, Influence of Cr and Fe on formation of α-Al_2O_3 from γ-Al_2O_3, J. Am. Ceram. Soc. 57 (8) (1974) 361–371.
[16] B.E. Yoldas, Thermal stablization of an active alumina and effect of dopants on the surface area, J. Mater. Sci. 11 (1976) 465–470.
[17] M. Machida, K. Eguchi, H. Arai, Preparation and characteristics of large-surface-area $BaO{\cdot}6H_2O$, Bull. Chem. Soc. Jpn. 61 (1988) 3659–3665.
[18] J.L. Mcardle, G.L. Messing, Transformation, microstructure development and densification in α-Fe_2O_3-seeded boehmite-derived alumina, J. Am. Ceram. Soc. 76 (1) (1993) 214–222.
[19] Y. Saito, T. Takei, S. Hayashi, A. Yasumori, K. Okada, Effect of amorphous and crystalline SiO_2 additives on γ-Al_2O_3-to-α-Al_2O_3 phase transitions, J. Am. Ceram. Soc. 81 (8) (1998) 2197–2200.
[20] F.W. Dynys, J.W. Halloran, Alpha alumina formation in alum-derived gamma alumina, J. Am. Ceram. Soc. 65 (9) (1982) 442–448.